TECHNICAL ARTICLE

Structure of triplite $LiFeSO_4F$ powder synthesized through an ambient two-step solid-state route

F.-F. Ma, J.-W. Mao, G.-Q. Shao,[a] S.-H. Fan, C. Zhu, A.-L. Zhang, G.-Z. Xie, J.-N. Gu, and J.-L. Yan
State Key Laboratory of Advanced Technology for Materials Synthesis and Processing, Wuhan University of Technology, 122 Luoshi Road, Wuhan 430070, China

(Received 31 March 2017; accepted 6 December 2017)

The triplite $LiFeSO_4F$ displays both the highest potential ever reported for an Fe-based compound, as well as a comparable specific energy with that of popular $LiFePO_4$. The synthesis is still a challenge because the present approaches are connected with long time, special equipments or organic reagents, etc. In this work, the triplite $LiFeSO_4F$ powder was synthesized through an ambient two-step solid-state route. The reaction process and phase purity were analyzed, coupled with structure refinement and electrochemical test. © *2018 International Centre for Diffraction Data*.
[doi:10.1017/S0885715618000040]

Key words: $LiFeSO_4F$, triplite, fluorosulfate, solid-state synthesis

I. INTRODUCTION

Three polymorphs of $LiMSO_4F$ fluorosulfates crystallize in triplite (M = Fe and Mn; monoclinic, *C2/c*) (Ati *et al.*, 2011, 2012a; Barpanda *et al.*, 2011a; Tripathi *et al.*, 2012, 2013; Lee and Park, 2014; Kim *et al.*, 2015; Kim and Kang, 2017), tavorite (M = Fe, Co, Ni, and Mg; triclinic, $P\bar{1}$) (Sebastian *et al.*, 2002; Ati *et al.*, 2010; Salanne *et al.*, 2012; Tripathi *et al.*, 2012; Jalem *et al.*, 2014; Sobkowiak *et al.*, 2014; Eriksson *et al.*, 2015), and sillimanite (M = Zn; orthorhombic, *Pnma*) (Barpanda *et al.*, 2011b; Tripathi *et al.*, 2012) structures. They are being extensively explored for using as cathodes (M = Fe, Mn, Co, and Ni) and electrolytes (M = Zn and Mg) in Li-ion batteries. Their solid solutions (Barpanda *et al.*, 2010, 2011a; Ramzan *et al.*, 2010; Cai *et al.*, 2011; Radha *et al.*, 2012; Tripathi *et al.*, 2012) adopt one of three isostructures or just mixed phases varying with compositions and synthesis conditions.

The fluorosulfate family is explored because of the following reasons. (a) The popular olivine $LiFePO_4$ phosphate has a redox potential of 3.45 V (Padhi *et al.*, 1997) and ionic conductivity of 2×10^{-9} S cm^{-1} at 147 °C with one-dimensional (1D) Li-ion diffusion (Amin *et al.*, 2007). To increase the ionic conductivity and alter dimensionality of Li^+ transport in this cathode material, the fluoride anion is incorporated to produce a 3D tavorite $LiFePO_4F$ fluorophosphate (2.8 V; 0.6–5.4×10^{-7} S cm^{-1} at 27–50 °C) (Ramesh *et al.*, 2010; Prabu *et al.*, 2012; Chen *et al.*, 2014). (b) Two methods are induced to compensate the unfavorable decrease of potential. The first is using other redox couple with a higher potential (e.g. V^{3+}/V^{4+}, 4.2 V) to replace Fe^{2+}/Fe^{3+} (Barker *et al.*, 2005). The second is to constitute a different polyanion moiety, e.g. Li_2FeSiO_4 orthosilicate (3.1 V) (Girish and Shao, 2015) and $LiFeSO_4F$ fluorosulfate with the potential of 3.6 V (7×10^{-11} S cm^{-1} at 25 °C and 4×10^{-6} S cm^{-1} at 147 °C) for tavorite (Ati *et al.*, 2010; Recham *et al.*, 2010; Yahia *et al.*, 2012) or 3.9 V for triplite (Ati *et al.*, 2011, 2012a; Barpanda *et al.*, 2011a; Yahia *et al.*, 2012). The last one displays both the highest potential ever reported for an Fe-based compound, as well as a comparable specific energy (588 Wh/kg) with that of $LiFePO_4$ (587 Wh/kg) (Ati *et al.*, 2012a).

The triplite $LiMSO_4F$ (M = Fe and Mn) can be synthesized by ambient direct solid-state (Radha *et al.*, 2012; Kim *et al.*, 2015; Kim and Kang 2017), pressure-controlled solid-state [e.g. autoclave (Ati *et al.*, 2011; Barpanda *et al.*, 2011a; Ati *et al.*, 2012a), vacuum (Liu *et al.*, 2011), or vacuum hot-pressing (Dong *et al.*, 2013)], extended solvothermal (Tripathi *et al.*, 2012), microwave solvothermal (Tripathi *et al.*, 2013), spark plasma sintering (Ati *et al.*, 2012a), ball-milling (Ati *et al.*, 2012a), and ionothermal (Barpanda *et al.*, 2011a) (only for M = Mn) methods. Several unit-cell parameters for triplite $LiFeSO_4F$ were reported (Ati *et al.*, 2011; Tripathi *et al.*, 2012, 2013; Kim *et al.*, 2015; Kim and Kang, 2017). We find till now (dated to October 30, 2017) one ***Crystallographic Information File*** (CIF), i.e. ICSD 187799 (Tripathi *et al.*, 2013), has been deposited in the *Inorganic Crystal Structure Database* (ICSD), Germany. The corresponding triplite $LiFeSO_4F$ was obtained through a microwave solvothermal route in an autoclave using tetraethylene glycol (TEG) as a reaction medium.

In this work, the triplite $LiFeSO_4F$ powder was synthesized through an ambient two-step solid-state route. The reaction process analysis, phase determination/refinement, galvanostatic cycling and cyclic voltammetry tests were performed.

II. EXPERIMENTAL

A. Sample preparation

The white $FeSO_4 \cdot H_2O$ powder (labeled as OS150_60) was pre-synthesized by heating commercial $FeSO_4 \cdot 7H_2O$ (99^+ wt%) at 150 °C for 60 min in argon. Then $FeSO_4 \cdot H_2O$ and LiF (99^+ wt%) mixture, with the stoichiometric ratio of

[a]Author to whom correspondence should be addressed. Electronic mail: gqshao@whut.edu.cn

$LiFeSO_4F$, was ball-milled with zirconia balls for 2 h in alcohol (99^+ wt%), dried at 60 °C for 12 h in vacuum, and formed into pellets. Pellets were kept in alumina crucibles and calcined once or twice in argon. After ball-milling, three series of brownish gray powders were obtained: (i) in a $FeSO_4 \cdot H_2O$/LiF mole ratio of 1 : 1 for 45 min at different temperatures (400, 450, or 500 °C); (ii) at 450 °C for 45 min in different ratios (1 : 1, 1 : 1.05, or 1 : 1.1 mol%); (iii) at 450 °C in a ratio of 1 : 1.05 in different holding time (45, 45 + 90, or 45 + 225 min), while the last two samples were calcined twice at the same temperature and well ground between. The corresponding samples were thus labeled as S400_45_1.0, S450_45_1.05, and S450_45 + 90_1.05 and so on.

B. Characterization

The reaction process of $FeSO_4 \cdot H_2O$/LiF (1 : 1, mol%) was studied by TG-DSC-MS (STA 449F3 & QMS403 C Aëolos, Netzsch Co. Ltd, Germany) from room temperature (RT) to 600 °C. Mass spectrometer monitored all of the possible gases such as H_2O, SO_3, SO_2, SO, O_2, F_2, H_2S, and HF. Phase analysis ($5° \le 2\theta \le 80°$) was carried out by XRD (RU-200B/D/Max-rB, Rigaku Co. Ltd, Japan) at a scan rate of 10°/min. Crystal structure determination ($5° \le 2\theta \le 140°$) was carried out using Cu$K\alpha$ radiation ($\lambda_{\alpha 1} = 1.54060$ Å, 40 kV, 40 mA) with a diffractometer (D8 Adv., Bruker Co. Ltd, Germany) in flat plate $\theta/2\theta$ geometry at 0.0194303°/s. Testing conditions included a divergence slit of 1.0 mm, an antiscatter slit of 7.39 mm, a primary soller slit of 2.5°, a second soller slit of 2.5°, and a detector slit of 12.27 mm. The structure refinement and quantitative analysis of phases were performed by Rietveld method implemented in GSAS/EXIGUI software (Larson *et al.*, 2004) using the model of $(Li1, Fe1)_{8f}(Li2, Fe2)_{8f}\{S_{8f}[O_{8f}]_4\}F_{8f}$ (Tripathi *et al.*, 2013). The $LiFeSO_4F$ electrode and coin-type cell were prepared using the same method as $LiFePO_4F$ (Chen *et al.*, 2014). Galvanostatic cycling was performed between 1.5 and 4.5 V using a CT2001A tester (Wuhan Land Electronics Co., Ltd., China) in a constant-current mode at 0.05 C. Cyclic voltammetry analysis was carried out between 2.0 and 4.5 V vs. Li/Li^+ at 0.1 mV s^{-1} using a CHI660e system (Shanghai Chenhua Instr. Co. Ltd, China).

III. RESULTS AND DISCUSSION

A. Reaction process $FeSO_4 \cdot H_2O$/LiF mixture

Figure 1 shows TG-DSC and MS spectra of the $FeSO_4 \cdot H_2O$/LiF mixture from RT to 600 °C. The parallel DSC tests for three times between 420 and 530 °C are shown together. The weight loss of −9.1 wt% ranging from 250 to 350 °C and the endothermic peak at 303 °C [Figure 1(a)], as well as ion current peak of H_2O evolving at 292 °C [Figure 1(b)] can be attributed to the loss of H_2O from $FeSO_4 \cdot H_2O$. The rest water was removed at higher temperature which can be seen from the MS result (cf. theoretical loss of −10.6 wt%). At the same time, the tavorite $LiFeSO_4F$ (tavorite abbreviated as tav and triplite as tri in the text, see later) forms by a topotactic reaction of $FeSO_4 \cdot H_2O$ with

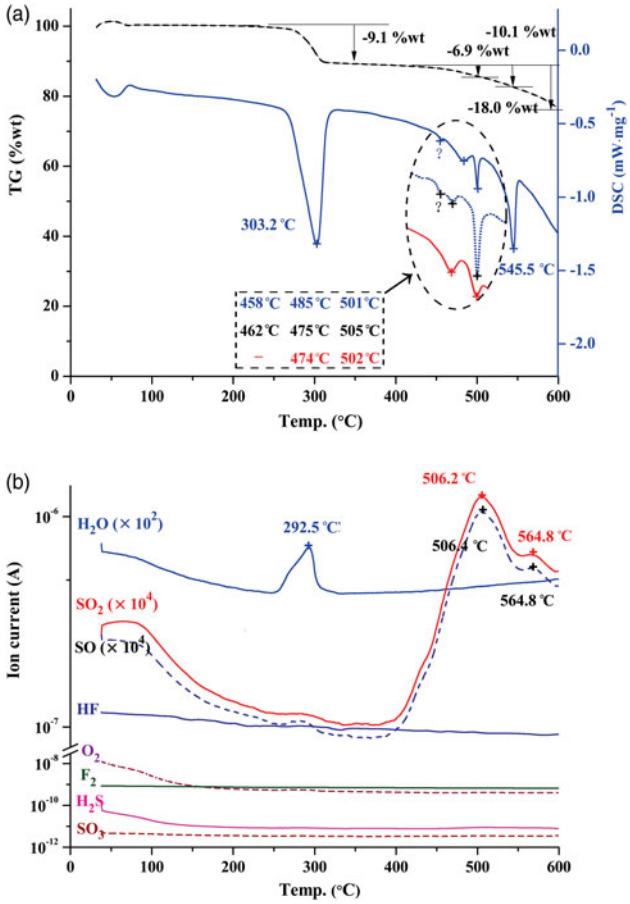

Figure 1. (Colour online) TG-DSC (a) and MS (b) spectra of the $FeSO_4 \cdot H_2O$/LiF mixture in argon from RT to 600 °C. The parallel DSC tests for three times between 420 and 530 °C are shown together.

LiF (Ati *et al.*, 2010).

$$FeSO_4 \cdot H_2O + LiF \xrightarrow{303\,°C,Ar} \text{tav-}LiFeSO_4F + H_2O \uparrow \quad (1)$$

The endothermic peak around 474–485 °C is corresponding to the thermodynamically favored transformation from tav- to tri-$LiFeSO_4F$. The peaks in parallel tests at 458–462 °C (labeled by question marks) are incognizable for the moment which disappear in the third test [Figure 1(a)].

$$\text{tav-}LiFeSO_4F \xrightarrow{474-485\,°C,\,Ar} \text{tri-}LiFeSO_4F \quad (2)$$

The calculated configurational enthalpy (ΔH), entropy (ΔS) and free energy change (ΔG) for the tav- to tri-$LiFeSO_4F$ transformation are 2.12 ± 0.79 kJ mol^{-1}, 0.01153 kJ mol^{-1} K^{-1}, and -1.32 ± 0.79 (25 °C)/-6.79 ± 0.79 kJ mol^{-1} (500 °C), respectively. The positive ΔH means endothermic. The $T\Delta S$ arising from disorder is enough to overcome the positive ΔH, thus ΔG becomes more exothermic at higher temperature (vs. RT) to promote synthesis process (Radha *et al.*, 2012).

The tri-$LiFeSO_4F$ has been synthesized at 250 °C for 14 days in autoclave (Tripathi *et al.*, 2012), at 350 °C for 1 h in microwave autoclave (Tripathi *et al.*, 2013), at 300 °C for 72 h in autoclave (Ati *et al.*, 2011), and at 400 °C for 1 h by a direct solid-state approach (Kim *et al.*, 2015; Kim and

https://doi.org/10.1017/S0885715618000040 Published online by Cambridge University Press

Kang, 2017). Considering the thermodynamical, kinetic, and synthetic condition within experimental error, the deductive transformation temperature around 474–485 °C is reasonable. Based on the TG-DSC-MS analysis, the optimized condition to synthesize highly pure tri-$LiFeSO_4F$ in this work is set for two-step calcination.

The endothermic peak around 501–505 °C (−6.9 wt% loss), as well as ion current peaks of SO_2 and SO evolving at 506 °C can be attributed to the decomposition of tri-$LiFeSO_4F$.

$$\text{tri-LiFeSO}_4\text{F} \xrightarrow{501\,^\circ\text{C, Ar}} \frac{3-x}{12}\text{Fe}_2(\text{SO}_4)_3 + \frac{3+x}{12}\text{Fe}_2\text{O}_3 + \text{LiF} + \frac{x}{2}\text{SO}_2\uparrow + \frac{1-x}{4}\text{SO}\uparrow\ (0 < x \le 1) \quad (3)$$

If decomposition were completed, the weight loss would be −18.0 wt%. The "SO" is not a stable product that its appearance is most likely the result of fragmentation in MS (Ati *et al.*, 2010). The analysis result does not appear to be affected whether there was "SO" released.

The endothermic peak at 546 °C corresponds to the eutectic temperature of $Fe_2(SO_4)_3$/LiF mixture, considering that their melting points are 480 °C and 845 °C, respectively. The latter is usually used as a component of molten salts. The ion current peaks of SO_2 and SO evolving at 565 °C may be because of two kinds of gases releasing continuously in the melt via Eq. (3). The possibility of $Fe_2(SO_4)_3$ decomposition is excluded considering its thermodynamics (Majzlan *et al.*, 2005) and no SO_3 releases.

MS tests show that there are H_2O, SO_2, and SO released at high temperature. Gases found or deduced by other researchers such as H_2S (Ati *et al.*, 2010), HF (Ati *et al.*, 2010), and F_2 (Guo *et al.*, 2014) have not been detected. This means the final reaction products should be highly pure or major tri-$LiFeSO_4F$ with tiny $Fe_2(SO_4)_3$, Fe_2O_3, and LiF [Eq. (3)].

B. Phase identification and optimization

Figure 2 shows XRD patterns for three series of powders prepared from mixtures of $FeSO_4 \cdot H_2O$ (pre-synthesized from $FeSO_4 \cdot 7H_2O$) and LiF in different conditions. Powders of Serie iii were tested at a scan rate of 0.0194303°/s, others at 0.1667°/s (10°/min). Results show that pure $FeSO_4 \cdot H_2O$ (OS150_60) is obtained by calcining $FeSO_4 \cdot 7H_2O$ at 150 °C for 60 min in argon. For powders of Serie i [Figure 2(a)], the main phase of tri-$LiFeSO_4F$ is obtained using $FeSO_4 \cdot H_2O$/LiF (1 : 1 mol%) for 45 min at 400, 450, or 500 °C while the minor phase is Fe_2O_3. The purity of tri-$LiFeSO_4F$ in S450_45_1.0 (93 ± 3 wt%) is higher than that in S400_45_1.0 (87 ± 3 wt%) and S500_45_1.0 (85 ± 3 wt%).

For powders of Serie ii [Figure 2(b)], while synthesizing at 450 °C for 45 min in different ratios (1 : 1, 1 : 1.05, or 1 : 1.1 mol%), adding a little excessive LiF can effectively suppress the decomposition of reaction products [Eq. (3)]. The purity of tri-$LiFeSO_4F$ in S450_45_1.05 (97.3 ± 1.5 wt%) is higher than that in S450_45_1.0 (93 ± 3 wt%) and S450_45_1.1 (94 ± 3 wt%).

Two-step solid-state route is then performed at 450 °C in a ratio of 1 : 1.05 in different holding time (45 min, 45 + 90 min, or 45 + 225 min), producing powders of Serie iii [Figure 2(b)]. The last two samples (S450_45 + 90_1.05 and S450_45 + 225_1.05) were calcined twice at the same temperature and well ground between. The sample S450_45 + 90_1.05 attains the highest purity of tri-$LiFeSO_4F$ phase (98.1 ± 1.5 wt%) which are better than the two-step synthesized S450_45 + 225_1.05 (96.8 ± 1.5 wt%) and the one-step synthesized S450_45_1.05 (97.3 ± 1.5 wt%).

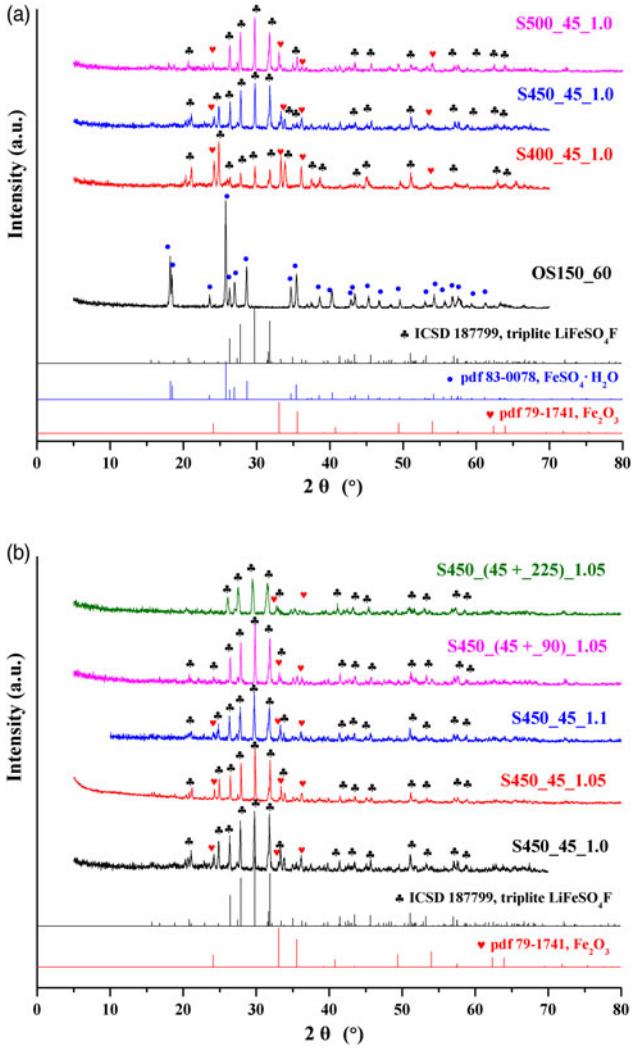

Figure 2. (Colour online) XRD patterns for three series of powders prepared from mixtures of $FeSO_4 \cdot H_2O$ (OS150_60) and LiF in different conditions: (i) in a mole ratio of 1 : 1 for 45 min at 400, 450, or 500 °C (S400_45_1.0, S450_45_1.0, and S500_45_1.0); (ii) at 450 °C for 45 min in a ratio of 1 : 1, 1 : 1.05, or 1 : 1.1 (S450_45_1.0, S450_45_1.05, and S450_45_1.1); (iii) at 450 °C in a ratio of 1 : 1.05 for 45, 45 + 90, or 45 + 225 min (S450_45_1.05, S450_45 + 90_1.05, and S450_45 + 225_1.05). Patterns for Serie i are shown in Figure 2(a). Patterns for Series ii and iii are shown in Figure 2(b).

All of the above samples can match tri-$LiFeSO_4F$ well without signal of tavorite. The final reaction products are highly pure or major tri-$LiFeSO_4F$ with tiny Fe_2O_3, $Fe_2(SO_4)_3$, and LiF (the latter two are amorphous), also confirmed by TG-DSC-MS test. Phases found or deduced by other researchers such as $FeSO_4$ (Liu *et al.*, 2011; Kim and Kang, 2017), FeS_2 (Recham *et al.*, 2010), $Li_2Fe(SO_4)_2$ (Ati *et al.*, 2012a; Kim and Kang, 2017), Li_2SO_4 (Guo *et al.*, 2014; Kim *et al.*, 2015; Kim and Kang, 2017), and Fe_3O_4 (Kim *et al.*, 2015; Kim and Kang, 2017) have not been detected in this work.

https://doi.org/10.1017/S0885715618000040 Published online by Cambridge University Press

Compared with the published investigations, this work has its distinctions: (i) shorter time, cf. 14 days (Tripathi *et al.*, 2012); (ii) simplified equipments, cf. autoclave (Ati *et al.*, 2011; Tripathi *et al.*, 2012, 2013) or microwave (Tripathi *et al.*, 2013); (iii) none organic reagents, cf. TEG (Tripathi *et al.*, 2012, 2013) or 1-ethyl-3-methylimidazolium-*bis*-trifluoromethylsulfonyl-imide ionic liquid (Ati *et al.*, 2011); (iv) two-step, carbon-free, and solid-state calcination, cf. one-step with impurities (Kim *et al.*, 2015) or one-step using sucrose ($C_{12}H_{22}O_{11}$) and poly-vinylidene fluoride (Kim and Kang, 2017). Particularly, there is one CIF file of tri-$LiFeSO_4F$ deposited in ICSD till now (ICSD 187799, dated to October 30, 2017) (Tripathi *et al.*, 2013). The reported triplite phase was obtained through a microwave solvothermal route in an autoclave using TEG as a reaction medium, being under a more rigorous condition.

C. Structure refinement and electrochemical test

Figure 3 shows the final observed, calculated, and difference profiles of the tri-$LiFeSO_4F$ structure (S450_45 + 90_1.05) via Rietveld refinement (see the online supplementary material). The inset shows the magnified section in the range of 35–65°. The Li^+-ion migration channels in the directions of [0 1 0] were shown in Figure 4(a) and in the directions of [1 0 1] shown were in Figure 4(b), respectively. Agreement indices (R_p, R_{wp}, and R_F^2) and goodness-of-fit (χ^2) in different Li/Fe occupancies were shown in Figure 4(c). Table I lists Rietveld refinement parameters of the tri-$LiFeSO_4F$ structure. Results show the Rietveld refinement converges with acceptable goodness-of-fit ($\chi^2 = 1.01$) and agreement indices (R_p = 1.25%, R_{wp} = 1.61%, R_{exp} = 1.60%, and R_F^2 = 13.9%). The fit results do not show any anomalies. The obtained structural and thermal parameters are reasonable and in full accord with ICSD 187799 (Tripathi *et al.*, 2013), but with some discrepancies to another model (Ati *et al.*, 2011). The MO_4F_2 (M = Fe, Li) octahedra are alternatively composed of F–F and O–O atoms. They share edges with each other forming two crystallographically zigzag chains along the directions of [0 1 0] and [1 0 1] (Yahia *et al.*, 2012). Two chains are connected by sharing F–O edges. The F atoms are in a *cis*-arrangement,

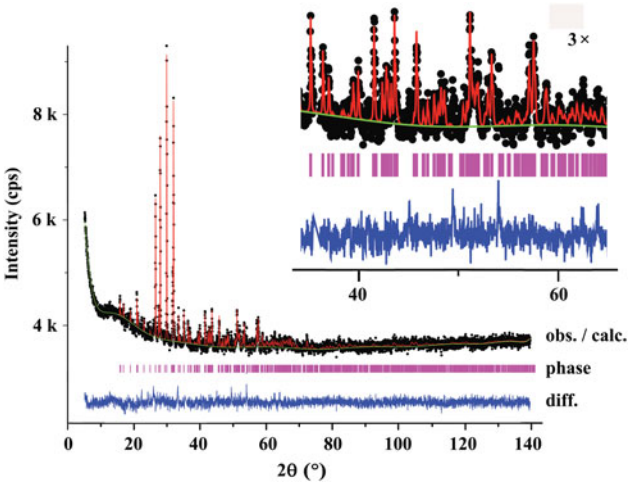

Figure 3. (Colour online) Final observed (dots), calculated (line), and difference profiles of the tri-$LiFeSO_4F$ structure via Rietveld refinement. The inset shows the magnified section in the range of 35–65°.

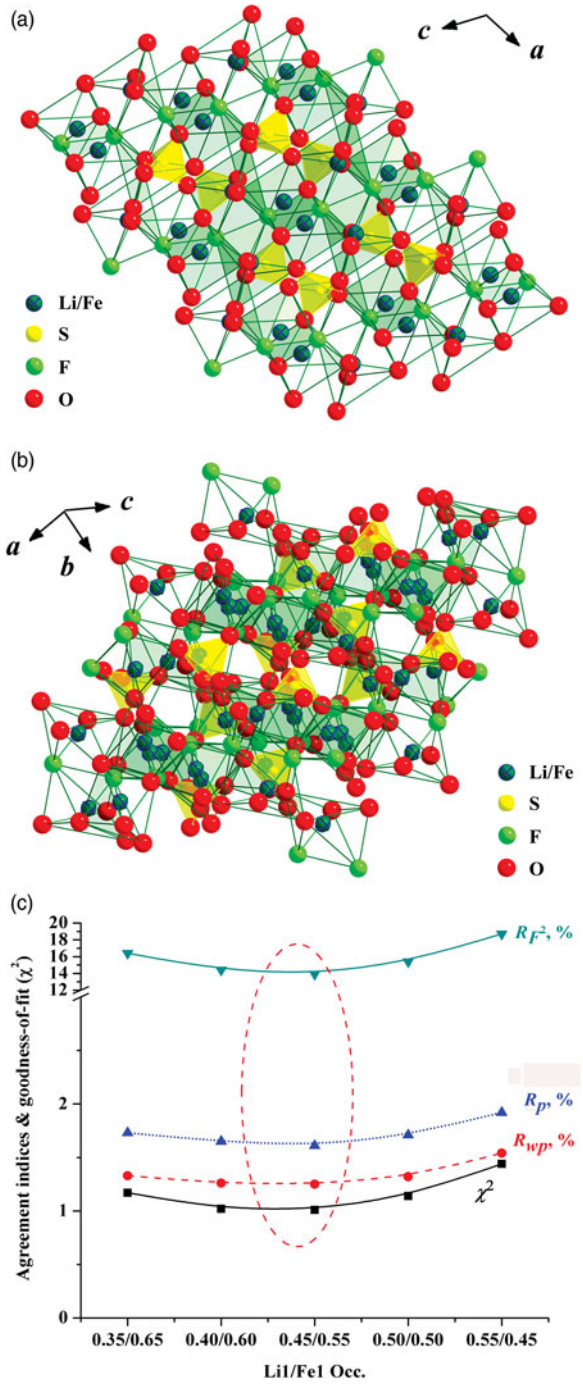

Figure 4. (Colour online) The Li^+-ion migration channels in the directions of [0 1 0] (a) and [1 0 1] (b), respectively. Agreement indices (R_p, R_{wp}, and R_F^2) and goodness-of-fit (χ^2) in different Li/Fe occupancies (c).

in contrast with the corner-shared tavorite isomorph (*trans* F−F). The SO_4 tetrahedra only share corners with other polyhedral (Chung *et al.*, 2012). The move in the [0 1 0] direction is partly restricted, unlike the tav-$LiFeSO_4F$ and resulted in a modest conductivity. There is significant disorder of Li and Fe on two sites [Figure 4(c)], while Li has a preference toward site 2 [0.450(6)−Li1/0.550(6)−Li2] and Fe toward site 1 [0.550(6)−Fe1/0.450(6)−Fe2]. But Li and Fe atoms are distributed in a 50–50 proportion in the tav-$LiFeSO_4F$ (Recham *et al.*, 2010). The entropy associated with the disordered nature of Li and Fe sites results in triplite being the

https://doi.org/10.1017/S0885715618000040 Published online by Cambridge University Press

TABLE I. Rietveld refinement parameters of the tri-$LiFeSO_4F$ structure.

Ions	Type	Wyckoff	x	y	z	Occ.	U_{iso} (Å^2)
Li^+/Fe^{2+}	Li1/Fe1	8*f*	0.6458 (8)	0.8965 (17)	0.8493 (10)	0.450 (6)/0.550 (6)	0.009 (2)
Li^+/Fe^{2+}	Li2/Fe2	8*f*	0.9474 (10)	0.2467 (20)	−0.0012 (14)	0.550 (6)/0.450 (6)	0.010 (3)
S^{6+}	S1	8*f*	0.3290 (11)	0.5909 (19)	0.1977 (14)	1	0.012 (1)
F^-	F1	8*f*	0.9858 (13)	0.3917 (20)	0.6119 (14)	1	0.017 (2)
O^{2-}	O1	8*f*	0.2185 (10)	0.6373 (20)	0.2015 (11)	1	0.011 (5)
O^{2-}	O2	8*f*	0.5758 (10)	0.5314 (16)	0.1368 (13)	1	0.011 (5)
O^{2-}	O3	8*f*	0.6887 (8)	0.4184 (20)	0.4141 (11)	1	0.019 (5)
O^{2-}	O4	8*f*	0.6391 (16)	0.7694 (12)	0.3594 (20)	1	0.013 (6)
χ^2	R_p	R_{wp}	R_{exp}	R_F^2	N_{obs}	$N_{constr.}$	
1.01	1.25%	1.61%	1.60%	13.9%	674	10	

Space group: *C2/c* (No.15); monoclinic; $Z = 8$; $M_r = 177.84$; $\rho_{cal.} = 3.3128$ g cm^{-3}.
$a = 13.0367(4)$ Å; $b = 6.3976(1)$ Å; $c = 9.8425(6)$ Å; $\beta = 119.6876(17)$; $V = 713.15(2)$ Å^3.

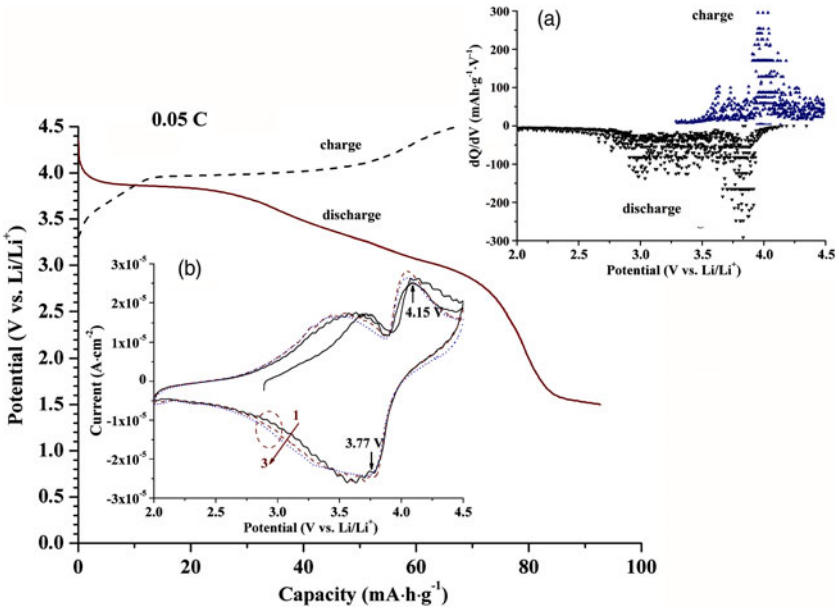

Figure 5. (Colour online) Charge/discharge profile of the tri-$LiFeSO_4F$ cell in the first cycle at 0.05 C. The inset (a) and (b) show the corresponding differential capacity plot and cyclic voltammogram in which cycle numbers are indicated, respectively.

thermodynamically preferred polymorph of $LiFeSO_4F$ (Radha *et al.*, 2012; Tripathi *et al.*, 2012, 2013). The intrinsic disorder in the precursor with hydroxyl groups, which decomposes upon solid-state conversion, favors the produce of triplite phase; and two-step calcination favors the transformation for hydroxyl groups to tavorite then to triplite, because it occurs very slowly (Tripathi *et al.*, 2013).

The voltage plateau on 3.9 V in the initial charge/discharge profile (Figure 5), and a pair of peaks in the differential capacity plot [the inset (a)] and cyclic voltammogram [the inset (b)] around 3.9 V are in good agreement with the Fe^{2+}/Fe^{3+} redox couple of tri-$LiFeSO_4F$. Results support those reported from charge/discharge profiles and differential capacity plots (Ati *et al.*, 2011, 2012a; Barpanda *et al.*, 2011a; Tripathi *et al.*, 2012, 2013; Kim *et al.*, 2015; Kim and Kang, 2017). The unexpected peak of 3.6 V [the insets (a) and (b)] may belong to the tavorite $LiFeSO_4F$ phase (Ati *et al.*, 2010; Recham *et al.*, 2010; Yahia *et al.*, 2012), even though the XRD had not detected it. Maybe this is because that the cyclic voltammogram test (none reports before) is more sensitive than the XRD. Besides, it seems to exist a trace $LiFeSO_4F_{1-x}(OH)_x$ phase with a couple centered at 3.3 V [the inset (a)], which could be attributed to the preparation process of powder (Ati *et al.*, 2012b), electrode, and cell with trace water from an external environment (Ati *et al.*, 2010). Deep research on the relationship among the phase purity, preparation, and electrochemical performance is under proceeding. The triplite has a higher operating potential than the tavorite because its vacancy destabilizing effect of Li^+-ion is larger. Under the edge-sharing geometry, the effect occurs because of strong $Fe^{3+}\cdots Fe^{3+}$ repulsive interaction around the vacancy (Ati *et al.*, 2012a; Chung *et al.*, 2012; Lee and Park, 2014).

IV. CONCLUSIONS

The Rietveld refinement of triplite $LiFeSO_4F$ explains the relation of high operating potential and modest conductivity to the structure, which is confirmed by the electrochemical test. The disorder of Li and Fe is also confirmed which is associated with entropy. The latter results in triplite being the thermodynamically preferred polymorph of $LiFeSO_4F$.

SUPPLEMENTARY MATERIAL

The supplementary material for this article can be found at https://doi.org/10.1017/S0885715618000040.

ACKNOWLEDGEMENTS

The authors gratefully acknowledge J.-H. Liu, D. Chen, and B. Li in their group, and Professor B.-L. Wu in GUT. This work was supported by Research Foundation of State Key Laboratory of Advanced Technology for Materials Synthesis and Processing, WUT, China (Grant Nos. 2015-KF-4 and 2016-KF-4).

APPENDIX

Further details of the crystal structure investigation may be obtained from FIZ Karlsruhe–Leibniz Institute for Information Infrastructure, 76344 Eggenstein–Leopoldshafen, Germany (https://www.fiz-karlsruhe.de/en/leistungen/kristallographie/kristallstrukturdepot.html) on quoting the appropriate CSD number (G.-Q. Shao *et al.*, The crystal structure of triplite $LiFeSO_4F$, CSD 432778, 2017.3.20).

Amin, R., Balaya, P., and Maier, J. (**2007**). "Anisotropy of electronic and ionic transport in $LiFePO_4$ single crystals," Electrochem. Solid-State Lett. **10**, A13–A16.

Ati, M., Walker, W. T., Djellab, K., Armand, M., Recham, N., and Tarascon, J.-M. (**2010**). "Fluorosulfate positive electrode materials made with polymers as reacting media," Electrochem. Solid-State Lett. **13**, A150–A153.

Ati, M., Melot, B. C., Chotard, J. N., Rousse, G., Reynaud, M., and Tarascon, J. M. (**2011**). "Synthesis and electrochemical properties of pure $LiFeSO_4F$ in the triplite structure," Electrochem. Commun. **13**, 1280–1283.

Ati, M., Sathiya, M., Boulineau, S., Reynaud, M., Abakumov, A., Rousse, G., Melot, B., Van Tendeloo, G., and Tarascon, J.-M. (**2012a**). "Understanding and promoting the rapid preparation of the triplite-phase of $LiFeSO_4F$ for use as a large-potential Fe cathode," J. Am. Chem. Soc. **134**, 18380–18387.

Ati, M., Sougrati, M. T., Rousse, G., Recham, N., Doublet, M. L., Jumas, J. C., and Tarascon, J. M. (**2012b**). "Single-step synthesis of $FeSO_4F_{1-y}OH_y$ ($0 \le y \le 1$) positive electrodes for Li-based batteries," Chem. Mater. **24**, 1472–1485.

Barker, J., Gover, R. K. B., Burns, P., and Bryan, A. (**2005**). "A symmetrical lithium-ion cell based on lithium vanadium fluorophosphate, $LiVPO_4F$," Electrochem. Solid-State Lett. **8**, A285–A287.

Barpanda, P., Recham, N., Chotard, J.-N., Djellab, K., Walker, W., Armand, M., and Tarascon, J.-M. (**2010**). "Structure and electrochemical properties of novel mixed $Li(Fe_{1-x}M_x)SO_4F$ (M=Co, Ni, Mn) phases fabricated by low temperature ionothermal synthesis," J. Mater. Chem. **20**, 1659–1820.

Barpanda, P., Ati, M., Melot, B. C., Rousse, G., Chotard, J.-N., Doublet, M.-L., Sougrati, M. T., Corr, S. A., Jumas, J.-C., and Tarascon, J.-M. (**2011a**). "A 3.90 V iron-based fluorosulphate material for lithium-ion batteries crystallizing in the triplite structure," Nat. Mater. **10**, 772–779.

Barpanda, P., Chotard, J. N., Delacourt, C., Reynaud, M., Filinchuk, Y., Armand, M., Deschamps, M., and Tarascon, J. M. (**2011b**). "$LiZnSO_4F$ made in an ionic liquid: a ceramic electrolyte composite for solid-state lithium batteries," Angew. Chem. Int. Ed. Engl. **50**, 2526–2531.

Cai, Y., Chen, G., Xu, X., Du, F., Li, Z., Meng, X., Wang, C., and Wei, Y. (**2011**). "First-principles calculations on the $LiMSO_4F$/MSO_4F (M=Fe, Co, and Ni) systems," J. Phys. Chem. C **115**, 7032–7037.

Chen, D., Shao, G.-Q., Li, B., Zhao, G.-G., Li, J., Liu, J.-H., Gao, Z.-S., and Zhang, H.-F. (**2014**). "Synthesis, crystal structure and electrochemical properties of $LiFePO_4F$ cathode material for Li-ion batteries," Electrochim. Acta **147**, 663–668.

Chung, S. C., Barpanda, P., Nishimura, S. I., Yamada, Y., and Yamada, A. (**2012**). "Polymorphs of $LiFeSO_4F$ as cathode materials for lithium ion batteries – a first principle computational study," Phys. Chem. Chem. Phys. **14**, 8678–8682.

Dong, J., Yu, X., Sun, Y., Liu, L., Yang, X., and Huang, X. (**2013**). "Triplite $LiFeSO_4F$ as cathode material for Li-ion batteries," J. Power Sources **244**, 716–720.

Eriksson, R., Sobkowiak, A., Ångström, J., Sahlberg, M., Gustafsson, T., Edström, K., and Björefors, F. (**2015**). "Formation of tavorite-type $LiFeSO_4F$ followed by *in situ* X-ray diffraction," J. Power Sources **298**, 363–368.

Girish, H.-N., and Shao, G.-Q. (**2015**). "Advances in high-capacity Li_2MSiO_4 (M=Mn, Fe, Co, Ni, . . .) cathode materials for lithium-ion batteries," RSC Adv. **5**, 98666–98686.

Guo, Z., Wei, Y., Zhang, D., Bie, X., Zhang, Y., Zhu, K., Zhang, R., and Chen, G. (**2014**). "Excellent thermal stability of tavorite Li_xFeSO_4F used as a cathode material for lithium ion batteries," RSC Adv. **4**, 64200–64203.

Jalem, R., Nakayama, M., and Kasuga, T. (**2014**). "Lithium ion conduction in tavorite-type $LiMXO_4F$ (M–X: AlP, MgS) candidate solid electrolyte materials," Solid State Ion. **262**, 589–592.

Kim, M., and Kang, B. (**2017**). "Highly-pure triplite 3.9 V-$LiFeSO_4F$ synthesized by a single-step solid-state process and its high electrochemical performance," Electrochim. Acta **228**, 160–166.

Kim, M., Jung, Y., and Kang, B. (**2015**). "High electrochemical performance of 3.9 V $LiFeSO_4F$ directly synthesized by a scalable solid-state reaction within 1 h," J. Mater. Chem. A **3**, 7583–7590.

Larson, A. C., and Von Dreele, R. B. (**2004**). "*General Structure Analysis System (GSAS) (Report LAUR 86-748)* (Los Alamos National Laboratory, Los Alamos, New Mexico).

Lee, S., and Park, S. S. (**2014**). "Comparative study of tavorite and triplite $LiFeSO_4F$ as cathode materials for lithium ion batteries: structure, defect chemistry, and lithium conduction properties from atomistic simulation," J. Phys. Chem. C **118**, 12642–12648.

Liu, L., Zhang, B., and Huang, X.-j. (**2011**). "A 3.9V polyanion-type cathode material for Li-ion batteries," Prog. Nat. Sci. Mater. Int. **21**, 211–215.

Majzlan, J., Navrotsky, A., Stevens, R., Donaldson, M., Woodfield, B. F., and Boerio-Goates, J. (**2005**). "Thermodynamics of monoclinic $Fe_2(SO_4)_3$," J. Chem. Thermodyn. **37**, 802–809.

Padhi, A. K., Nanjundaswamy, K. S., and Goodenough, J. B. (**1997**). "Phospho-olivines as positive-electrode materials for rechargeable lithium batteries," J. Electrochem. Soc. **144**, 1188–1194.

Prabu, M., Reddy, M. V., Selvasekarapandian, S., Rao, G. V. S., and Chowdari, B. V. R. (**2012**). "Synthesis, impedance and electrochemical studies of lithium iron fluorophosphate, $LiFePO_4F$ cathode," Electrochim. Acta **85**, 572–578.

Radha, A. V., Furman, J. D., Ati, M., Melot, B. C., Tarascon, J. M., and Navrotsky, A. (**2012**). "Understanding the stability of fluorosulfate Li-ion battery cathode materials: a thermochemical study of $LiFe_{1-x}Mn_xSO_4F$ ($0 \le x \le 1$) polymorphs," J. Mater. Chem. **22**, 24446–24452.

Ramesh, T. N., Lee, K. T., Ellis, B. L., and Nazar, L. F. (**2010**). "Tavorite lithium iron fluorophosphate cathode materials: phase transition and electrochemistry of $LiFePO_4F$-Li_2FePO_4F," Electrochem. Solid-State Lett. **13**, A43–A47.

Ramzan, M., Lebègue, S., and Ahuja, R. (**2010**). "Crystal and electronic structures of lithium fluorosulphate based materials for lithium-ion batteries," Phys. Rev. B: Condens. Matter **82**, 125101–125105.

Recham, N., Chotard, J.-N., Dupont, L., Delacourt, C., Walker, W., Armand, M., and Tarascon, J.-M. (**2010**). "A 3.6 V lithium-based fluorosulphate insertion positive electrode for lithium-ion batteries," Nat. Mater. **9**, 68–74.

Salanne, M., Marrocchelli, D., and Watson, G. W. (**2012**). "Cooperative mechanism for the diffusion of Li^+ ions in $LiMgSO_4F$," J. Phys. Chem. C **116**, 18618–18625.

Sebastian, L., Gopalakrishnan, J., and Piffard, Y. (**2002**). "Synthesis, crystal structure and lithium ion conductivity of $LiMgFSO_4$," J. Mater. Chem. **12**, 374–377.

Sobkowiak, A., Roberts, M. R., Häggström, L., Ericsson, T., Andersson, A. M., Edström, K., Gustafsson, T., and Björefors, F. (**2014**). "Identification of an intermediate phase, $Li_{1/2}FeSO_4F$, formed during electrochemical cycling of tavorite $LiFeSO_4F$," Chem. Mater. **26**, 4620–4628.

Tripathi, R., Popov, G., Ellis, B. L., Huq, A., and Nazar, L. F. (**2012**). "Lithium metal fluorosulfate polymorphs as positive electrodes for Li-ion batteries: synthetic strategies and effect of cation ordering," Energy Environ. Sci. **5**, 6238–6246.

Tripathi, R., Popov, G., Sun, X., Ryan, D. H., and Nazar, L. F. (**2013**). "Ultra-rapid microwave synthesis of triplite $LiFeSO_4F$," J. Mater. Chem. A **1**, 2990–2994.

Yahia, M. B., Lemoigno, F., Rousse, G., Boucher, F., Tarascon, J.-M., and Doublet, M.-L. (**2012**). "Origin of the 3.6 V to 3.9 V voltage increase in the $LiFeSO_4F$ cathodes for Li-ion batteries," Energy Environ. Sci. **5**, 9584–9594.